arXiv:0905.1704v2 [cond-mat.str-el] 12 Dec 2009

Orbital-Ordering Induces Structural Phase Transition and the Resistivity Anomaly in Iron Pnictides

Weicheng Lv, Jiansheng Wu, and Philip Phillips
Department of Physics, University of Illinois at Urbana-Champaign, 1110 West Green Street, Urbana, IL 61801

(Dated: December 12, 2009)

We attribute the structural phase transition (SPT) in the parent compounds of the iron pnictides to orbital ordering. Due to the anisotropy of the d_{xz} and d_{yz} orbitals in the xy plane, a ferro-orbital ordering makes the orthorhombic structure more energetically favorable, thus inducing the SPT. In this orbital-ordered system, the sites with orbitals that do not order have higher energies. Scattering of the itinerant electrons by these localized two-level systems causes a resistivity anomaly upon the onset of the SPT. The proposed orbital ordering also leads to the stripe-like anti-ferromagnetism and anisotropy of the magnetic exchanges. This model is quantitatively consistent with available experimental observations.

PACS numbers: 61.50.Ah, 71.70.Ej, 72.15.Qm

I. INTRODUCTION

The structural phase transition (SPT) from tetragonal to orthorhombic symmetry around $150\,\mathrm{K}^1$ is a ubiquitous feature in the parent compounds of the iron-based superconductors. Coincident with this transition is a resistivity anomaly (RA)[2] in which the resistivity turns up slightly before a sharp drop at exactly the onset temperature of the SPT, T_{SPT}. For the 1111-family, at a lower temperature, T_{SDW}, a stripe-like anti-ferromagnetic spin density wave (SDW) forms[3] on the distorted lattice of Fe atoms, with the spins being parallel along the shorter axis and anti-parallel along the longer axis. However, for the 122-family, the SDW develops at the same temperature as does the SPT, $T_{\mathrm{SDW}} = T_{\mathrm{SPT}}$[4]. In the 122-family[5], a single first-order transition obtains instead of two separate second-order transitions in the 1111-family. Upon doping, superconductivity (SC) occurs leading to a cessation of the SPT, RA and SDW[6,7]. Hence, all of these three phenomena should be closely related and share a universal mechanism. However, most theoretical work only focuses on the connections between the SDW and SC. The importance of the SPT and RA is somehow underestimated. The main objective of this paper is to explain the origin of the SPT and RA.

A common view[8,9,10,11] is that the SPT is driven by the onset of the stripe-like anti-ferromagnetism. Both first principles calculations[8,9] and Landau-Ginzburg modelings[10,11] have been used in this context. The fact that the two transitions are decoupled in the 1111-family is a limitation of this approach. Further, since the origin of the SPT in their scenario is spin based, the onset temperature should be sensitive to an external magnetic field. However, experiments have shown that varying the magnetic field leads to no change in the onset temperature of the SPT[2].

In this paper, we develop a microscopic theory of the SPT without involving the spin degrees of freedom. On our account, uneven occupations of the d_{xz} and d_{yz} orbitals make the orthorhombic crystal structure more energetically favorable, thus inducing the SPT. The operative mechanism driving this ferro-orbital-ordering transition is the lifting of the degeneracy between the d_{xz} and d_{yz} orbitals by the inter-site Coulomb repulsions. However, it should be noted that other important factors, such as spin-orbit interactions[12] and couplings to the displacements of ligand atoms (As), also contribute to this process. In fact, spin-orbit physics appears to lie at the heart of orbital ordering in the manganites[13]. While such physics is undoubtedly present in the pnictides[14,15], quantifying it would require a first-principles calculation of the relevant parameters. However, as our goal is to propose a simple mechanism that explains both the SPT and the resistivity anomaly, we focus on a more easily quantifiable approach to orbital ordering based instead on the Coulomb repulsion. Indeed, what our work indicates is that there is a rich set of models which can lead to orbital ordering in the pnictides. Our model is sufficiently simple and general that warrant its being taken seriously. The key insight gained from this study is not the detailed microscopic mechanism for this orbital-ordering-induced SPT, which is rather standard[13], but its direct consequence - a resistivity anomaly, which can be captured by our model in quantitative agreement with the experimental results [see Fig. 3(b)]. Furthermore, the stripe-like SDW and recently discovered anisotropy[16] of the magnetic exchanges naturally arise in our theory.

II. ORBITAL ORDERING

As being emphasized by pioneering earlier work[14], the orbital degrees of freedom are important in the iron pnictides, which are intrinsically multi-orbital systems. For the Fe atom located at the center of the tetrahedron of four neighboring As atoms, the five d orbitals are split into two groups, t_{2g} (d_{xy}, d_{xz}, d_{yz}) and e_g ($d_{x^2-y^2}$, $d_{3z^2-r^2}$). Three of the five orbitals, d_{xy}, $d_{x^2-y^2}$ and $d_{3z^2-r^2}$ are rotationally symmetric in the xy plane. So they are unlikely to have any effect on the SPT which is asymmetric in the xy plane. Then the only two possible candidates are the d_{xz} and d_{yz} orbitals. We propose the

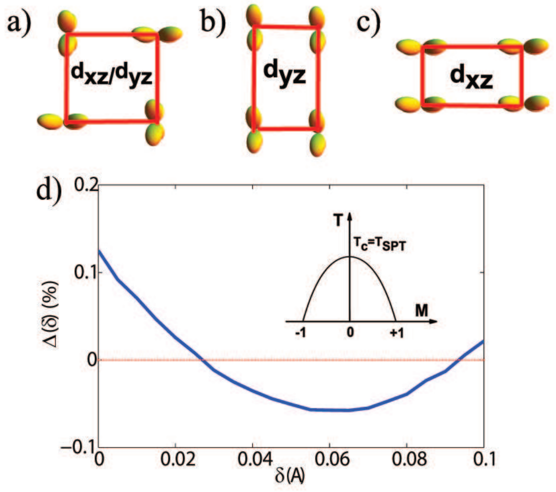

FIG. 1: (Color online) (a) Equal numbers of d_{xz} and d_{yz} with a square lattice configuration. (b) Entirely d_{yz} state with $a < b$. (c) Entirely d_{xz} state with $a > b$. d) Relative energy difference Δ between configurations (a) and (b), or (c), as a function of lattice distortion δ. (Inset: an Ising-type transition where the order parameter M is defined as the difference between the numbers of occupied d_{xz} and d_{yz} orbitals.)

following mechanism for the SPT, assuming these two orbitals are localized. At high temperature $T > T_{\rm SPT}$, d_{xz} and d_{yz} orbitals are degenerate, with equal numbers of electrons on both. A possible configuration is shown in Fig. 1(a), in which a square lattice is preferred. At low temperature, $T < T_{\rm SPT}$, there is a majority of either d_{xz} or d_{yz}. For d_{yz} orbitals, the Coulomb repulsion of two neighboring sites is stronger along the y-direction than along the x-direction, which leads to a rectangular lattice with $a < b$ as shown in Fig. 1(b), where a and b are unit lengths in the x and y direction, respectively. Similarly, when d_{xz} dominates, the system will form the configuration of Fig. 1(c), which is degenerate with (b) by a rotation of 90 degrees.

To demonstrate the viability of this mechanism, we need to compare the energies of configuration (a) and (b) in Fig. 1. For simplicity, only the nearest-neighbor Coulomb repulsions are considered,

$$U = \int d\boldsymbol{r}\, d\boldsymbol{r'} \frac{e^2}{|\boldsymbol{r}-\boldsymbol{r'}|} \left|\psi_\alpha(\boldsymbol{r}-\boldsymbol{R}_i)\right|^2 \left|\psi_\beta(\boldsymbol{r'}-\boldsymbol{R}_j)\right|^2 \quad (1)$$

where $\psi_\alpha(\boldsymbol{r}-\boldsymbol{R}_i)$ is the wave function of the α ($\alpha = d_{xz}, d_{yz}$) orbital electron at site $\boldsymbol{R}_i$. This integral can be evaluated by an importance-sampling Monte-Carlo method. In configuration (a), we choose $a = b = a_0 = 2.85$ Å, which is the typical experimental value[1] for the 1111-family. For configuration (b), we define the lattice distortion δ as $a = a_0 - \delta$, and set $b = a_0^2/a$ to keep the area of a unit cell constant. We calculate the relative energy difference

$$\Delta(\delta) = \frac{U_b(\delta) - U_a}{U_a} \quad (2)$$

as a function of δ, where U_a and U_b are energies of configurations (a) and (b) respectively. The results are shown in Fig. 1(d). For a lattice distortion 0.03 Å$< \delta <$ 0.09 Å, the rectangular lattice (b) or (c) is more energetically favorable. It is noted that this value is larger than the experimentally observed distortion of about 0.01 Å[1]. However, the localized states are probably neither d_{xz} nor d_{yz}, but some combinations of the d orbitals, or even involve hybridization with As p orbitals[17]. Thus the precise value of the distortion length can be smaller by taking these factors into account. As already mentioned, other possibilities may also induce this ferro-orbital ordering and the subsequent SPT. For example, Krüger *et. al*[14] derive a Kugel-Khomskii spin-orbital model and the resultant phase diagram does contain the same orbital configuration as proposed here. However, constructing the complete microscopic Hamiltonian that incorporates all the important physical processes requires a detailed knowledge of the relevant coupling parameters, which is currently unavailable. Thus the key point of our study is to put forth a simplified picture based on the coupling only to the Coulomb interaction in which the rectangular lattice with ferro-orbital ordering emerges spontaneously at low temperature because of its lower energy.

Our model allows us to make the following conclusion. Upon the onset of the phase transition, a lattice distortion breaks the degeneracy between d_{xz} and d_{yz}. By occupying either one of these two orbitals, the system forms a ferro-orbital-ordered state and lowers its energy. It is this orbital-driven Jahn-Teller effect that induces the SPT. Defining $M_i = \pm 1$ for site i occupied by d_{xz} and d_{yz} orbitals respectively, we can write down an effective Ising-type Hamiltonian for the SPT

$$H_{\rm SPT} = -J_{\rm SPT} \sum_{\langle i,j \rangle} M_i M_j \quad (3)$$

where $J_{\rm SPT}$ should be on the order of the transition temperature, $T_{\rm SPT}$. So the SPT belongs to the Ising universality class, as shown in the inset of Fig. 1(d), where the order parameter M is defined as $M = \sum_i M_i/N$.

Recently, angle-resolved photoemission experiments using a linear-polarized laser beam[18] show that at low temperature, the Fermi surface at the Brillouin zone center is dominated by a single d_{xz} or d_{yz} orbital, depending on the distortions. In their subsequent local-density approximation (LDA) calculations[18], it is found that the density of states of the d_{yz} orbitals with a lattice configuration of $a < b$ displays a peak around 0.5 eV from the chemical potential, which is just the localized state predicted in our SPT model. A recent optical measurement[19] also suggests evidences of the orbital ordering.

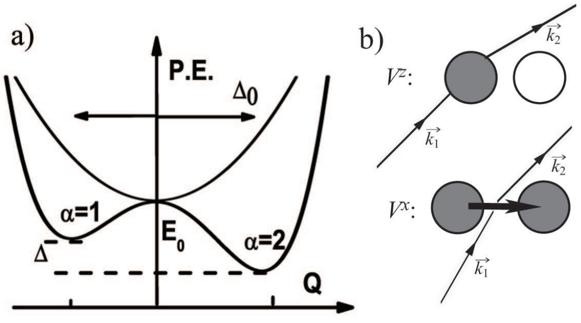

FIG. 2: (a) A schematic of a double-well potential, as the classical analog of the two-level system. (b) Two types of scattering processes between the itinerant electrons and the localized states. V^z: diagonal scattering; and V^x: off-diagonal scattering.

III. RESISTIVITY ANOMALY

The ferro-orbital-ordering-driven SPT mechanism has an important consequence, namely the resistivity anomaly. The essential physics is that of a Kondo problem. The scattering of the itinerant electrons off two otherwise degenerate orbitals, d_{xz} and d_{yz}, will be suppressed by the gap opening, which results in a sharp drop of the resistivity upon the onset of the SPT.

Above, T_{SPT}, the two d_{xz} and d_{yz} orbitals are degenerate. Below T_{SPT}, the occupancy of the electrons in d_{xz} and d_{yz} orbitals becomes unbalanced as a result of the distortion of the crystal to configuration (c) [or (b)] in Fig. 1. Thus, the electrons that remain in the d_{yz} (or d_{xz}) orbitals will have a higher energy and hence can lower their energy by jumping onto d_{xz} (or d_{yz}) orbitals. This process can be described by a localized two-level system. The classical analog, namely a double-well potential, is shown in Fig. 2(a). The corresponding Hamiltonian is given by

$$\begin{aligned} H_{\text{TLS}} &= \lambda_{\text{ps}} \sum_{\alpha} a^\dagger_\alpha a_\alpha + \frac{1}{2}\Delta \sum_{\alpha\beta} a^\dagger_\alpha \sigma^z_{\alpha\beta} a_\beta \\ &+ \frac{1}{2}\Delta_0 \sum_{\alpha\beta} a^\dagger_\alpha \sigma^x_{\alpha\beta} a_\beta \end{aligned} \tag{4}$$

where $a^\dagger_\alpha$ (a_α) creates (annihilates) an electron on orbital α and $\sigma^i_{\alpha\beta}$ is a Pauli matrix. We will choose an appropriate fictitious energy λ_{ps} to prevent the system from double occupancy. Δ is the energy splitting between the two levels and Δ_0 is the tunneling rate, as shown in Fig. 2(a). By a rotation of the spin axis, this system can be diagonalized and the gap between the two eigenstates is $E = \sqrt{\Delta_0^2 + \Delta^2}$.

As the parent compounds are actually metallic, there should be itinerant electrons present besides these localized states. These two can be coupled as in the framework of the localized-itinerant dichotomous models[17,20,21,22]. The starting Hamiltonian is[23]

$$\begin{aligned} H &= H_e + H_{\text{TLS}} + V && (5)\\ H_e &= \sum_{k\sigma} E_k c^\dagger_{k\sigma} c_{k\sigma} && (6)\\ V &= \sum_i \sum_{k_1\sigma_1, k_2\sigma_2} \sum_{\alpha\beta} c^\dagger_{k_2\sigma_2} V^i_{k_2k_1} c_{k_1\sigma_1}\, a^\dagger_\alpha \sigma^i_{\alpha\beta} a_\beta && (7) \end{aligned}$$

where H_e, H_{TLS} and V represent the Hamiltonians for the itinerant electrons, the single two-level system and the interactions between the two, respectively. There are two kinds of scattering processes as shown in Fig. 2(b). One is the diagonal scattering described by the V^z term, where the localized state remains on the same level. The other is the off-diagonal scattering initiated by the V^x term, where the localized state jumps onto the other level. V^y is in fact zero, as it breaks time-reversal symmetry. However, it should be noted that $V^y = 0$ does not hold for the renormalized vertex, since higher order terms are not necessarily local. We will also assume $V^z \gg V^x$ as proposed previously[23].

In fact, this system is very similar to the Kondo model, with the two orbitals d_{xz} and d_{yz} representing the up and down-spin states on the magnetic impurity. We are going to perform a similar scaling analysis following Ref. 23. We define the dimensionless couplings $v^i_{k_1k_2} = V^i_{k_1k_2} N_0$ where N_0 is the density of states at the Fermi level. Reducing the bandwidth from D_0 to D and evaluating the vertex corrections up to the leading order, we have the scaling equations

$$\frac{\partial v^s_{\alpha\beta}(u)}{\partial u} = -2i \sum_{ij} \sum_{\gamma} \epsilon^{ijs} v^i_{\alpha\gamma}(u) v^j_{\gamma\beta}(u) \tag{8}$$

where $v^i_{\alpha\beta}$ are defined as $v^i_{k_1k_2} = \sum f^\dagger_\alpha(\hat{k_1}) v_{\alpha\beta} f_\beta(\hat{k_2})$, with $f_\alpha(\hat{k})$ being a complete set of spherical harmonics, $f_\alpha(\hat{k}) = i^l Y^m_l(\theta_k, \phi_k)$, ϵ^{ijs} is the Levi-Civita symbol and $u = \ln(D/D_0)$. We can express $v^i_{\alpha\beta}$ using the Pauli matrices as $v^i_{\alpha\beta} = v^i \sigma^i_{\alpha\beta}$. Then the above scaling equations will be reduced to a set of coupled equations involving v^x, v^y and v^z. These equations can be solved by separating u into two regimes: (a) $v^y < v^x \ll v^z$ and (b) $v^y \simeq v^x < v^z$. In regime (a), the solutions are

$$\begin{aligned} v^x(u) &= v^x(0)\cosh\left[4v^z(0)u\right] && (9)\\ v^y(u) &= v^x(0)\sinh\left[4v^z(0)u\right] && (10)\\ v^z(u) &= v^z(0). && (11) \end{aligned}$$

In regime (b), we have

$$\left[v^z(u)\right]^2 - \left[v^x(u)\right]^2 = v_0^2, \tag{12}$$

where v_0 is scale invariant and $v^z(u)$ satisfies

$$u = -\frac{1}{4v^z(u)} + \ln\left[\frac{D_0}{k_{\text{B}}T_k}\right] \tag{13}$$

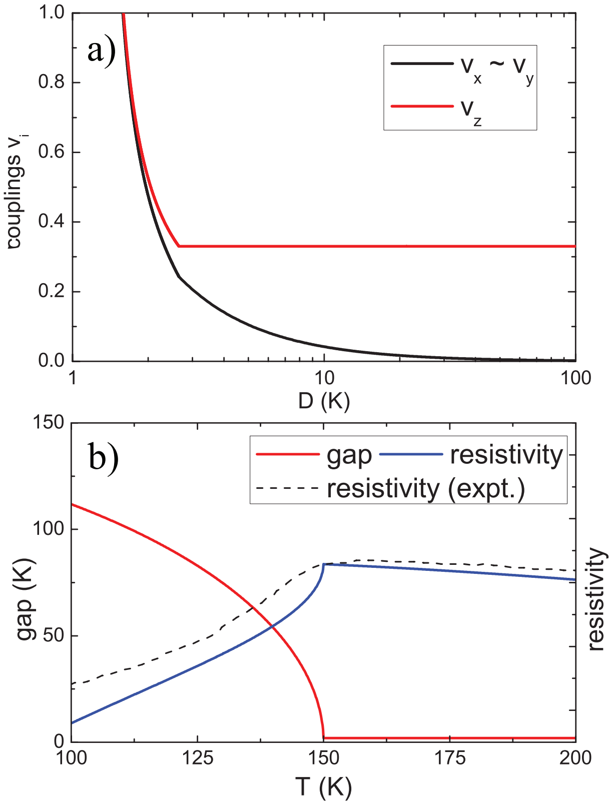

FIG. 3: (Color online) (a) Scaling of the coupling constants v^i with respect to bandwidth D. (b) Energy gap and resistivity as a function of temperature T. (The experimental data of resistivity are extracted from Ref.[2].) Setting the resistivity at $T = 150K$ of our model equal to that of the experiment was the only fitting parameter.

with the Kondo temperature T_k identified as

$$k_{\mathrm{B}}T_k = D_0 \left[\frac{v^x(0)}{4v^z(0)}\right]^{1/4v^z(0)} . \tag{14}$$

Using the parameters $v^z(0) = 0.33$, $v^x(0)/v^z(0) = 0.001$, $v^y(0) = 0$ and $D_0 = 665\,\mathrm{K}$[24], we obtained the scaling flows of v^x, v^y and v^z shown in Fig. 3(a), for $E = 0\,\mathrm{K}$. The corresponding Kondo temperature is $T_k = 1.24\,\mathrm{K}$. Reducing the bandwidth D, the system goes from weak to strong coupling. The resistivity due to the scattering of the two-level system can be calculated based on these renormalized vertices as in Ref. 24. At high temperature, we have two degenerate levels, d_{xz} and d_{yz}. When the temperature is reduced, the scattering from the states closer to the chemical potential increases, leading to a resistivity upturn of $\log T$[25] as in the Kondo model. However, upon the onset of the SPT, a gap opens between the two levels. If the bandwidth D is less than the gap E, the off-diagonal scattering is not allowed, since there are no states for the electrons to be scattered into. As a consequence, the scaling terminates at $D = E$. The electrons within the bandwidth E will no longer contribute to the resistivity. This is the mechanism behind the resistivity anomaly. Our result is shown in Fig. 3(b), which is in good qualitative agreement with experiment. We set the tunneling rate $\Delta_0 = 2\,\mathrm{K}$, and the energy splitting takes the form

$$\Delta(T) = \Delta(0)\sqrt{1 - \left(\frac{T}{T_{\mathrm{SPT}}}\right)^2} \tag{15}$$

where $\Delta(0) = T_{\mathrm{SPT}} = 150\,\mathrm{K}$ when $T < T_{\mathrm{SPT}}$. It should be noted that the overall behavior of the scaling flows and the resistivity are independent of the chosen parameters. This represents the explanation of the RA for the iron pnictides.

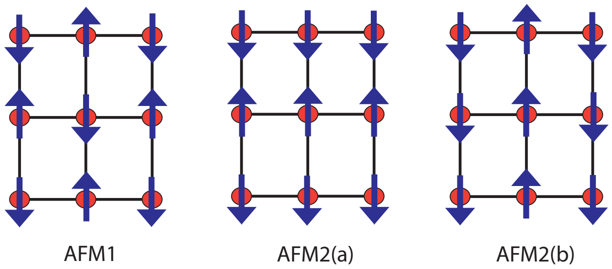

FIG. 4: (Color online) Different possible spin configurations on a distorted lattice with $a < b$, which corresponds to the case that d_{yz} is the majority orbital.

IV. ORBITAL DRIVEN MAGNETISM

Our model also offers a natural solution to the observed stripe-like anti-ferromagnetism. Before the SPT, we have an orbitally disordered state, in which the neighboring sites are occupied probabalistically by different orbitals. The resultant lack of overlap gives rise to a vanishing of any anti-ferromagnetic spin exchange and as a consequence no spin order. After the SPT, either d_{xz} or d_{yz} orbitals will dominate. Without loss of generality, we suppose that most sites are occupied by d_{yz}, as shown in Fig. 1(b). Due to the larger overlap of the wave functions on neighboring sites in the y-direction than that in the x-direction, the hopping integral t_b should be larger than t_a. For the nearest-neighbor spin exchange, $J_1 \sim t^2/U$, we have that $J_{1a} < J_{1b}$. So the spins on the longer axis have a stronger tendency to be aligned oppositely. The spin configuration AFM2(b) in Fig. 4 is not favored. As has been suggested[8,26], we can further introduce a next-nearest-neighbor exchange J_2. If $J_2 > J_{1a}/2$, which is very likely for a relatively small J_{1a}[14], AFM2(a) will have a lower energy than AFM1, as shown in Fig. 4, and emerge as the ground state at low temperature, which has already been confirmed by the experiments[3]. In contrast with other theories in which the SPT is induced by the spin degrees of freedoms, on this account, the formation of the SDW is actually a result of the ferro-orbital ordering accompanying the SPT.

In fact, we are able to construct a universal Hamiltonian describing both the SPT and SDW, with a spin-orbit coupling model[13,14,15],

$$\begin{aligned} H_{\rm SO} &= J_{\rm SPT}\sum_{\langle i,j\rangle} M_i M_j + \sum_{\langle\langle i,j\rangle\rangle} J_2\left(M_i,M_j\right)\boldsymbol{S}_i\cdot\boldsymbol{S}_j \\ &\quad +\sum_i J_{1x}\left(M_i,M_{i+\hat{x}}\right)\boldsymbol{S}_i\cdot\boldsymbol{S}_{i+\hat{x}} \\ &\quad +\sum_i J_{1y}\left(M_i,M_{i+\hat{y}}\right)\boldsymbol{S}_i\cdot\boldsymbol{S}_{i+\hat{y}} \qquad (16) \end{aligned}$$

where the spin exchanges are given by

$$\begin{aligned} J_{1x}\left(M_i,M_j\right) &= \delta_{M_i,M_j}\left(J_{1b}\delta_{M_i,1}+J_{1a}\delta_{M_i,-1}\right) \quad (17)\\ J_{1y}\left(M_i,M_j\right) &= \delta_{M_i,M_j}\left(J_{1a}\delta_{M_i,1}+J_{1b}\delta_{M_i,-1}\right) \quad (18)\\ J_2\left(M_i,M_j\right) &= \delta_{M_i,M_j}J_2 \quad (19) \end{aligned}$$

where M_i, representing the orbital degrees of freedom, is defined to be ± 1 for d_{xz} and d_{yz} respectively, as in Sec. II. Clearly, in this model, the spin order will not occur until the formation of the ferro-orbital ordering at $T_{\rm SPT}$, which is on the order of $J_{\rm SPT}$. Below $T_{\rm SPT}$, the spin degrees of freedom can be described by an anisotropic Heisenberg model, whose transition temperature to the spin-ordered state, T_s, would depend on the spin exchanges, J_{1a}, J_{1b} and J_2. If $T_S < T_{\rm SPT}$, we would have two separate second-order transitions, $T_{\rm SDW} = T_S < T_{\rm SPT}$, as in the case of the 1111-family. For the 122-family, which has a shorter Fe-Fe bond length, it is expected this would enhance the spin exchange J, likely leading to $T_S > T_{\rm SPT}$. But the SDW will not form before the SPT, since there is no spin exchange until the SPT obtains. So there is only one first-order transition, $T_{\rm SDW} = T_{\rm SPT}$.

Furthermore, this anisotropic Heisenberg model has also been proposed on experimental grounds[16] to fit the spin-wave spectrum seen in the inelastic neutron scattering data. Our theory gives a direct explanation for the observed anisotropy of magnetic exchanges. Note their results[16] do rely on a negative J_1^a, which is not obtained by our simple model. However, this difficulty can overcome by introducing a Hund's coupling between these localized spins and itinerant electrons,

$$H_K = -\frac{J_H}{2}\sum_{i,\nu\nu'}\boldsymbol{S}_i\cdot c^{\dagger}_{i\nu}\boldsymbol{\sigma}_{\nu\nu'}c_{i\nu'} \qquad (20)$$

where $\boldsymbol{\sigma}_{\nu\nu'}$ are the Pauli matrices. The hopping of the itinerant electrons with this Hund's coupling will give rise to an effective ferromagnetic coupling[27,28,29] between neighboring spins. After taking this into account, we will eventually have the spins on the shorter axis coupled ferromagnetically. The full details of this model are the subject of a future study.

V. FINAL REMARKS

To conclude, we have proposed that the SPT and RA in the iron pnictides are due to the opening of a gap between two otherwise degenerate orbitals. While our mechanism for the structural phase transition is a standard Jahn-Teller distortion driven by a minimization of the Coulomb repulsion, the key point of this paper is that the resulting simple two-level system can resolve the previously unexplained resistivity anomaly. The mechanism proposed here is independent of an applied magnetic field as is seen experimentally[2]. Only in a ferro-orbital-ordered state after the SPT does the stripe-like SDW form. This is the reason why these three phenomena, SPT, RA and SDW, are closely related and almost always coincide with one another. In doped materials, extra electrons or holes will break the uneven occupations of d_{xz} and d_{yz}, thus diminishing the Jahn-Teller effect. So the SPT, RA and SDW will all become less pronounced and shift to lower temperature, eventually vanishing at some critical doping. These are all observed experimentally, lending credence to our model.

After this work was posted on arXiv, several similar papers[30,31] appeared, based on the same orbital physics we utilized here, which supports our theory that the orbital ordering is the driving mechanism for the SPT, RA and SDW.

Acknowledgments

We thank the NSF under Grant No. DMR-0605769 for partial funding of this work and Frank Krüger for his insightful remarks.

---

[1] T. Nomura, S. W. Kim, Y. Kamihara, M. Hirano, P. V. Sushko, K. Kato, M. Takata, A. L. Shluger, and H. Hosono, Supercond. Sci. Technol. **21**, 125028 (2008).

[2] J. Dong, H. J. Zhang, G. Xu, Z. Li, G. Li, W. Z. Hu, D. Wu, G. F. Chen, X. Dai, J. L. Luo, Z. Fang, and N. L. Wang, Europhys. Lett. **83**, 27006 (2008).

[3] C. de la Cruz, Q. Huang, J. W. Lynn, J. Li, W. Ratcliff II, J. L. Zarestky, H. A. Mook, G. F. Chen, J. L. Luo, N. L. Wang, and P. Dai, Nature **453**, 899 (2008).

[4] Q. Huang, Y. Qiu, W. Bao, M. A. Green, J. W. Lynn, Y. C. Gasparovic, T. Wu, G. Wu, and X. H. Chen, Phys. Rev. Lett. **101**, 257003 (2008).

[5] A. I. Goldman, D. N. Argyriou, B. Ouladdiaf, T. Chatterji, A. Kreyssig, S. Nandi, N. Ni, S. L. Bud'ko, P. C. Canfield, and R. J. McQueeney, Phys. Rev. B **78**, 100506(R) (2008).

[6] J. Zhao, Q. Huang, C. de la Cruz, S. Li, J. W. Lynn, Y. Chen, M. A. Green, G. F. Chen, G. Li, Z. Li, J. L. Luo, N. L. Wang, and P. Dai, Nature Materials, **7**, 953 (2008).

[7] H. Luetkens, H.-H. Klauss, M. Kraken, F. J. Litterst, T. Dellmann, R. Klingeler, C. Hess, R. Khasanov, A. Am-

ato, C. Baines, M. Kosmala, O. J. Schumann, M. Braden, J. Hamann-Borrero, N. Leps, A. Kondrat, G. Behr, J. Werner, and B. Büchner, Nature Materials, **8**, 305 (2009).

[8] T. Yildirim, Phys. Rev. Lett. **101**, 057010 (2008).

[9] P. V. Sushko, A. L. Shluger, M. Hirano, and H. Hosono, Phys. Rev. B **78**, 172508 (2008).

[10] C. Xu, M. Müller, and S. Sachdev, Phys. Rev. B **78**, 020501(R) (2008).

[11] C. Fang, H. Yao, W.-F. Tsai, J. P. Hu, and S. A. Kivelson, Phys. Rev. B **77**, 224509 (2008).

[12] K. I. Kugel and D. I. Khomskii, Sov. Phys. JETP **52**, 501 (1981).

[13] Y. Tokura and N.Nagaosa, Science, **288**, 462 (2000).

[14] F. Krüger, S. Kumar, J. Zaanen, and J. van den Brink, Phys. Rev. B **79**, 054504 (2009).

[15] R. R. P. Singh, arXiv:0903.4408 (unpublished).

[16] J. Zhao, D. T. Adroja, D.-X. Yao, R. Bewley, S. Li, X. F. Wang, G. Wu, X. H. Chen, J. Hu, and P. Dai, Nature Physics **5**, 555 (2009).

[17] J. Wu, P. Phillips, and A. H. Castro Neto, Phys. Rev. Lett. **101**, 126401 (2008).

[18] T. Shimojima, K. Ishizaka, Y. Ishida, N. Katayama, K. Ohgushi, T. Kiss, M. Okawa, T. Togashi, X.-Y. Wang, C.-T. Chen, S. Watanabe, R. Kadota, T. Oguchi, A. Chainani, and S. Shin, arXiv:0904.1632 (unpublished).

[19] A. Akrap, J. J. Tu, L. J. Li, G. H. Cao, X. A. Xu, and C. C. Homes, Phys. Rev. B **80**, 180502(R) (2009).

[20] J. Dai, Q. Si, J.-X. Zhu, and E. Abrahams, Proc. Natl. Acad. Sci. **106**, 4118 (2009).

[21] S.-P. Kou, T. Li, and Z.-Y. Weng, Europhys. Lett. **88**, 17010 (2009).

[22] J. Wu and P. Phillips, arXiv:0901.3538 (unpublished).

[23] K. Valádar and A. Zawadowski, Phys. Rev. B **28**, 1564 (1983); **28**, 1582 (1983); **28**, 1596 (1983).

[24] S. Katayama, S. Maekawa, and H. Fukuyama, J. Phys. Soc. Jpn. **56**, 697 (1987).

[25] J. Dai, G. Cao, H.-H. Wen, and Z. Xu, arXiv:0901.2787 (unpublished).

[26] Q. Si and E. Abrahams, Phys. Rev. Lett. **101**, 076401 (2008).

[27] C. Zener, Phys. Rev. **82**, 403 (1951).

[28] P. W. Anderson and H. Hasegawa, Phys. Rev. **100**, 675 (1955).

[29] P.-G. de Gennes, Phys. Rev. **118**, 141 (1960).

[30] C.-C. Lee, W.-G. Yin, and W. Ku, arXiv:0905.2957 (unpublished).

[31] A. M. Turner, F. Wang, and A. Vishwanath, Phys. Rev. B **80**, 224504 (2009).